Zirconium Complexes of 9-Phenyl-9-borataanthracene. Synthesis, Structural Characterization, and Reactivity

Rip A. Lee, Rene J. Lachicotte, and Guillermo C. Bazan*,†

Contribution from the Department of Chemistry, University of Rochester, Rochester, New York 14627-0216

Received August 4, 1997. Revised Manuscript Received April 23, 1998

Abstract: Lithium 9-phenyl-9-borataanthracene (**3**·Li(THF)$_x$, $x = 2$ or 3) is obtained quantitatively from the deprotonation of 9-phenyl-9,10-dihydro-9-borataanthracene (**6**) with LiTMP (TMP = 2,2,6,6-tetramethylpiperidide) in THF. A comparison of the crystallographically determined structures of **6** and **3**·Li(TMEDA) (TMEDA = *N*,*N*,*N*′,*N*′-tetramethylethylenediamine) highlights the effects of charge and delocalization on the heterocyclic framework. The reaction of **3**·Li(THF)$_2$ with Cp*ZrCl$_3$ (Cp* = C_5Me_5) and Cp*ZrMe$_2$Cl affords the novel complexes (AnB-Ph)Cp*ZrCl$_2$ (**4**) (AnB-Ph = 9-phenyl-9-borataanthracene) and (AnB-Ph)Cp*ZrMe$_2$ (**5**), respectively. The crystallographically determined molecular structure of **4** resembles a bent metallocene with a tetrahedral disposition of ligands around zirconium. The borataanthracene ligand bends significantly (approx 16°) to avoid steric contacts with the Cp*ZrCl$_2$ core. The angle of the exocyclic phenyl substituent relative to the anthracene unit remains nearly invariant at 62° for **6**, **3**·Li(TMEDA), and **4**, suggesting that the steric envelope around boron prevents an optimum orientation for orbital overlap between boron and the π-system of the phenyl ring. Treatment of **5** with B(C_6F_5)$_3$ gives [(AnB-Ph)Cp*ZrMe][MeB(C_6F_5)$_3$] (**7**). Reaction of **4** with methylaluminoxane (MAO) and 1 atm of ethylene produces a mixture of low molecular weight 1-alkenes, 2-alkenes, and 2-alkyl-1-alkenes, whereas the reaction of **7** with ethylene gives low molecular weight polyethylene. Reactions of **4**/MAO and **7** with 1-tridecene were carried out to determine the fate of 1-alkenes generated using **4**/MAO/C_2H_4 and to delineate the role of the activator. The complex (C_5H_5B-Ph)Cp*ZrCl$_2$ (**8**) is obtained by reaction of Cp*ZrCl$_3$ with Li[C_5H_5B-Ph]. A comparison of the reactivity of **8**/MAO/C_2H_4 against that of **4**/MAO/C_2H_4 highlights, for the first time, the effect of sterics on the stability of catalysts supported by boratacyclic ligands.

Introduction

Electron-deficient bent metallocenes of the general type [Cp$_2$MR]$^+$[NCA]$^-$ (M = Ti, Zr, or Hf; Cp = η^5-C_5H_5, cyclopentadienyl; R = alkyl or hydride; NCA = noncoordinating anion) constitute a major class of homogeneous olefin polymerization catalysts. These systems have been the subject of several reviews.[1] Indeed, the wealth of information gleaned from nearly two decades of research has led to a good understanding of the mechanistic details involved in olefin insertion chemistry,[2] the nature of the active species,[3] the role of co-activators,[4] and the requisite structural features for stereoselective catalysis.[5]

Intense research efforts have centered on the design and synthesis of sterically modified metallocenes of diverse architectures. In particular, the advent of *ansa*-metallocenes marked an explosive growth of investigations into the stereospecific polymerization of propylene.[6,7] The structural correlation of the catalyst with its reactivity, and with the resultant polymer microstructure, has been the subject of much work,[8] and innovative strategies for the design of chiral metallocenes continue to emerge in the literature.[9] Collectively, the impor-

† Current address: Department of Chemistry, University of California, Santa Barbara, CA 93106.

(1) (a) *Transition Metals and Organometallics as Catalysts for Olefin Polymerization*; Kaminsky, W., Sinn, H., Eds.; Springer-Verlag: Berlin, 1988. (b) *Ziegler Catalysts*; Fink, G., Mülhaupt, R., Brintzinger, H.-H., Eds.; Springer-Verlag: Berlin, 1995. (c) Mohring, P. C.; Coville, N. J. *J. Organomet. Chem* **1994**, *479*, 1. (d) Huang, J.; Rempel, G. L. *Prog. Polym. Sci.* **1995**, *20*, 459. (e) Kaminsky, W.; Arndt, M. In *Applied Homogeneous Catalysis with Organometallic Compounds*; Cornils, B., Hermann, W. A., Eds.; VCH: Weinheim, Germany, 1995. (f) Bochmann, M. *J. Chem. Soc., Dalton Trans.* **1996**, 255.

(2) (a) Bierwagen, E. P.; Bercaw, J. E.; Goddard, W. A., III. *J. Am. Chem. Soc.* **1994**, *116*, 1481. (b) Shapiro, P. J.; Schaefer, W. P.; Labinger, J. A.; Bercaw, J. E.; Cotter, W. D. *J. Am. Chem. Soc.* **1994**, *116*, 4623. (c) Gilchrist, J. H.; Bercaw, J. E. *J. Am. Chem. Soc.* **1996**, *118*, 12021.

(3) (a) Eisch, J. J.; Piotrowski, A. M.; Brownstein, S. K.; Gabe, E. J.; Lee, F. L. *J. Am. Chem. Soc.* **1985**, *107*, 7219. (b) Hlatky, G. G.; Turner, H. W.; Eckman, R. R. *J. Am. Chem. Soc.* **1989**, *111*, 2798. (c) Jordan, R. F. *Adv. Organomet. Chem.* **1991**, *32*, 325. (d) Yang, X.; Stern, C. L.; Marks, T. J. *J. Am. Chem. Soc.* **1991**, *113*, 3623. (e) Bochmann, M.; Lancaster, S. J. *Organometallics* **1993**, *12*, 633.

(4) (a) Jordan, R. F.; LaPointe, R. E.; Bajgur, C. S.; Echols, S. F.; Willett, R. *J. Am. Chem. Soc.* **1987**, *109*, 4111. (b) Horton, A. D.; Orpen, A. G. *Organometallics* **1991**, *10*, 3910. (c) Yang, X.; Stern, C. L.; Marks, T. J. *J. Am. Chem. Soc.* **1994**, *116*, 10015. (d) Bochmann, M. *Angew. Chem., Int. Ed. Engl.* **1992**, *31*, 1181. (e) Bliemeister, J.; Hagendorf, W.; Harder, A.; Heitmann, B.; Schimmel. I.; Schmedt, E.; Schnuchel, W.; Sinn, H.; Tikwe, L.; von Thienen, N.; Urlass, K.; Winter, H.; Zarnacke, O. In *Ziegler Catalysts*; Fink, G., Mülhaupt, R., Brintzinger, H.-H., Eds.; Springer-Verlag: Berlin, 1995. (f) Jia, L.; Yang, X.; Stern, C. L.; Marks, T. J. *Organometallics* **1997**, *16*, 842.

(5) (a) Kaminsky, W.; Külper, K.; Brintzinger, H.-H.; Wild, F. R. W. P. *Angew. Chem., Int. Ed. Engl.* **1985**, *34*, 507. (b) Ewen, J. A.; Jones, R. L.; Razavi, A.; Ferrara, J. D. *J. Am. Chem. Soc.* **1988**, *110*, 6255. (c) Brintzinger, H.-H.; Fischer, D.; Mülhaupt, R.; Rieger, B.; Waymouth, R. M. *Angew. Chem., Int. Ed. Engl.* **1995**, *24*, 1143.

(6) (a) Schnutenhaus, H.; Brintzinger, H.-H. *Angew. Chem., Int. Ed. Engl.* **1979**, *18*, 777. (b) Wild, F. R. W. P.; Zsolnai, L.; Huttner, G.; Brintzinger, H.-H. *J. Organomet. Chem.* **1982**, *232*, 233. (c) Wild, F. R. W. P.; Wasiucionek, M.; Huttner, G.; Brintzinger, H.-H. *J. Organomet. Chem.* **1985**, *288*, 63.

(7) Coates, G. W.; Waymouth, R. M. *Science* **1995**, *267*, 217.

S0002-7863(97)02651-6 CCC: $15.00
Published on Web 06/09/1998

tance of metallocene catalysts is demonstrated by their rising impact in the future direction of polyolefin technology.[10]

An alternative approach for catalyst design involves the electronic modification of the metal center by preparing metallocene-like complexes with ligands other than cyclopentadienyl. One class of compounds includes the "constrained geometry" metallocenes which contain, in addition to the reduced steric volume, a less electron-donating amide functionality which enhances the electrophilicity of the metal.[11] The use of chelating bis-amides has also given rise to catalysts with novel reactivities.[12] The formal replacement of a monoanionic Cp with dianionic π-donor ligands has also been exploited. Thus, bent metallocenes containing "Cp-like" ligands such as dicarbollide,[13] trimethylenemethane,[14] and borollide[15] have been constructed, some of which display reactivities similar to those of standard metallocenes.[16]

The use of boratabenzenes (C_5H_5B-L, L = pendant group) as ancillary ligands for early transition metals, though limited thus far, is of growing interest.[17] In particular, these ligands have been used to construct precursors for homogeneous olefin polymerization catalysts with structures and electronic properties similar to those of standard group 4 metallocenes.[18] It appears that the electron density at the metal center can be controlled by the orbital overlap between B and L. The rich chemistry of boratabenzene metal complexes[19] has spanned over two decades since the landmark discovery of (C_5H_5B-Ph)CpCo in 1970.[20] The elegant synthesis of uncomplexed Li[C_5H_5B-Ph],[21] and subsequently other alkali metal boratabenzenes,[22] has provided a more versatile strategy for the synthesis of new boratabenzene-containing metal complexes. Further applications of this heterocyclic ligand may be anticipated, especially as new variations of the ligand framework continue to develop.[23]

As mentioned above, the salient feature of boratabenzene ligands is their ability to tune the electron density at the metal center and, hence, to modulate the reactivity of the metal complex. Solutions of [C_5H_5B-N(iPr)$_2$]$_2$ZrCl$_2$ (**1**) with methylaluminoxane (MAO) polymerize ethylene to give high molecular weight polyethylene (PE).[18a] In sharp contrast, solutions of [C_5H_5B-Ph]$_2$ZrCl$_2$ (**2**) with MAO give 2-alkyl-1-alkenes under similar reaction conditions. Differences in reactivities were attributed to differences in the rates of β-hydrogen elimination due to changing the exocyclic substituent.[18b] Strong π-donation of the pendant dialkylamino group with boron[24] results in the coordination of boratabenzene to zirconium in an η^5-pentadienyl fashion. However, when the π-interaction is weaker, the boratabenzene is best described as an η^6-bound, aromatic ligand. Overall, these features render the zirconium atom in **1** less electrophilic than that in **2**.

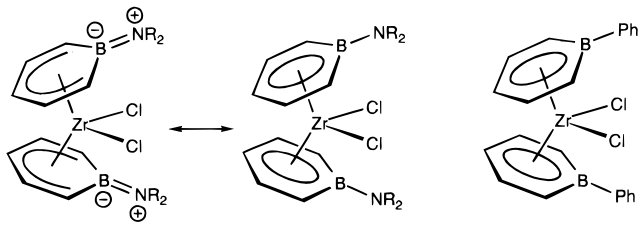

(**1**) (**2**)

Structural variations of the boratabenzene ligand may be achieved by extending the framework around boron. In this context, we became interested in the 9-phenyl-9-borataanthracene anion, first claimed by Jutzi,[25] since its use as a ligand in a metal complex has not been explored.[26] The analogies between this benzannulated derivative and phenylboratabenzene should be similar to those between Cp and the sterically larger Cp* (Cp* = C_5Me_5) and fluorenyl analogues. The sterically more protecting framework of borataanthracene should be useful in stabilizing reactive and/or coordinatively unsaturated species.[27]

The modified synthesis and the complete characterization of lithium 9-phenyl-9-borataanthracene are described in the first part of this paper.[28] The use of this ligand as a boratabenzene or Cp equivalent is shown by the synthesis of the novel complexes (AnB-Ph)Cp*ZrX$_2$ (AnB-Ph = 9-phenyl-9-borataan-

(8) (a) Halterman, R. L. *Chem. Rev.* **1992**, *92*, 965. (b) Erker, G.; Nolte, R, Aul, R.; Wilker, S.; Krüger, C, Noe, R. *J. Am. Chem. Soc.* **1991**, *113*, 7594. (c) Mengele, W.; Diebold, J.; Troll, C.; Roll, W.; Brintzinger, H.-H. *Organometallics* **1993**, *12*, 1931. (d) Ellis, W. W.; Hollis, T. K.; Odendirk, W.; Whelan, J.; Ostrander, R.; Rheingold, A. L.; Bosnich, B. *Organometallics* **1993**, *12*, 4391. (e) Grossman, R. B.; Tsai, J. C.; Davis, W. M.; Gutiérrez, A.; Buchwald, S. B. *Organometallics* **1994**, *13*, 3892. (f) Chen, Y. X.; Rausch, M. D.; Chien, J. C. W. *J. Organomet. Chem.* **1994**, *487*, 29. (g) Kaminsky, W.; Rabe, O.; Schauwienold, A. M.; Schupfner, G. U.; Hanss, J.; Kopf, J. *J. Organomet. Chem.* **1995**, *497*, 181.

(9) (a) Erker, G., Psiorz, C.; Fröhlich, R.; Grehl, M.; Krüger, C.; Noe, R.; Nolte, M. *Tetrahedron* **1995**, *51*, 4347. (b) Giardello, M. A.; Eisen, M. S.; Stern, C. L.; Marks, T. J. *J. Am. Chem. Soc.* **1995**, *117*, 12114. (c) Diamond, G. M.; Jordan, R. F.; Petersen, J. L. *J. Am. Chem. Soc.* **1996**, *118*, 8024. (d) Alt, H. G.; Zenk, R. *J. Organomet. Chem.* **1996**, *526*, 295. (e) Herzog, T. A.; Zubris, D. L.; Bercaw, J. E. *J. Am. Chem. Soc.* **1996**, *118*, 11988. (f) Nifant′ev, I. E.; Ivchenko, P. V. *Organometallics* **1997**, *16*, 713.

(10) (a) Thayer, A. M. *Chem. Eng. News* **1995** (Sept 11), 15. (b) Montagna, A. A. *CHEMTECH* **1995** (Oct), 44.

(11) (a) Shapiro, P. J.; Bunel, E. E.; Schaefer, W. P.; Bercaw, J. E. *Organometallics* **1990**, *9*, 867. (b) Lai, S. Y.; Wilson, J. R.; Knight, G. W.; Stevens, J. C.; Chuan, P. S. U.S. Patent 5,272,236, 1993. (c) Okuda, J. *Chem. Ber.* **1990**, *123*, 1649.

(12) (a) Scollard, J. D.; McConville, D. H. *J. Am. Chem. Soc.* **1996**, *118*, 10008. (b) Tinkler, S.; Deeth, R. J.; Duncalf, D. J.; McCamley, A. *Chem. Commun.* **1996**, 2623.

(13) (a) Crowther, D. J.; Baenziger, N. C.; Jordan, R. F. *J. Am. Chem. Soc.* **1991**, *113*, 1455. (b) Kreuder, C.; Jordan, R. F.; Zhang, H. *Organometallics* **1995**, *14*, 2993.

(14) (a) Bazan, G. C.; Rodriguez, G.; Cleary, B. P. *J. Am. Chem. Soc.* **1994**, *116*, 2177. (b) Rodriguez, G.; Bazan, G. C. *J. Am. Chem. Soc.* **1995**, *117*, 10155.

(15) Quan, R. W.; Bazan, G. C.; Kiely, A. F.; Schaefer, W. P.; Bercaw, J. E. *J. Am. Chem. Soc.* **1994**, *116*, 4459.

(16) (a) Bazan, G. C.; Donnelly, S. J.; Rodriguez, G. *J. Am. Chem. Soc.* **1995**, *117*, 2671. (b) Kowal, C. M.; Bazan, G. C. *J. Am. Chem. Soc.* **1996**, *118*, 10317.

(17) Service, R. F. *Science* **1996**, *271*, 1363.

(18) (a) Bazan, G. C.; Rodriguez, G.; Ashe, A. J., III; Al-Ahmad, S.; Müller, C. *J. Am. Chem. Soc.* **1996**, *118*, 2291. (b) Bazan, G. C.; Rodriguez, G.; Ashe, A. J., III; Al-Ahmad, S.; Kampf, J. W. *Organometallics* **1997**, *16*, 2492.

(19) Herberich, G. E.; Ohst, H. *Adv. Organomet. Chem.* **1986**, *25*, 199.

(20) Herberich, G. E.; Greiss, G.; Heil, H. F. *Angew. Chem., Int. Ed. Engl.* **1970**, *9*, 805.

(21) Ashe, A. J., III; Shu, P. *J. Am. Chem. Soc.* **1971**, *93*, 1804.

(22) Herberich, G. E.; Becker, H. J.; Carsten, K.; Engelke, C.; Koch, W. *Chem. Ber.* **1976**, *109*, 2382.

(23) (a) Herberich, G. E.; Schmidt, B.; Englert, U.; Wagner, T. *Organometallics* **1993**, *12*, 2891. (b) Herberich, G. E.; Schmidt, B.; Englert. U. *Organometallics* **1995**, *14*, 471. (c) Herberich, G. E.; Englert, U.; Schmidt, M. U.; Standt, R. *Organometallics* **1996**, *15*, 2707. (d) Hoic, D. A.; Davis, W. M.; Fu, G. C. *J. Am. Chem. Soc.* **1995**, *117*, 8480. (e) Qiao, S.; Hoic, D. A.; Fu, G. C. *J. Am. Chem. Soc.* **1996**, *118*, 6329.

(24) (a) Ashe, A. J., III; Kampf, J. W.; Müller, C.; Schneider, M. *Organometallics* **1996**, *15*, 387. (b) Ashe, A. J., III; Kampf, J. W.; Waas, J. R. *Organometallics* **1997**, *16*, 163.

(25) Jutzi, P. *Angew. Chem., Int. Ed. Engl.* **1972**, *11*, 53.

(26) For related work with the 9-mesityl-9-borataanthracene anion, see: (a) van Veen, R.; Bickelhaupt, F. *J. Organomet. Chem.* **1972**, *43*, C41. (b) van Veen, R.; Bickelhaupt, F. *J. Organomet. Chem.* **1974**, *74*, 393. (c) van Veen, R.; Bickelhaupt, F. *J. Organomet. Chem.* **1974**, *77*, 153. (d) Finocchiaro, P.; Recca, A.; Bottino, F. A.; Bickelhaupt, F.; van Veen, R.; Schenk, H.; Schagen, J. D. *J. Am. Chem. Soc.* **1980**, *102*, 5594. (e) Lapin, S. C.; Brauer, B.-E.; Schuster, G. B. *J. Am. Chem. Soc.* **1984**, *106*, 2092.

(27) For a lucid account of how sterics affects the stability of electrophilic organometallic species, see: Piers, W. E.; Shapiro, P. J.; Bunel, E. E.; Bercaw, J. E. *Synth. Lett.* **1990**, 74.

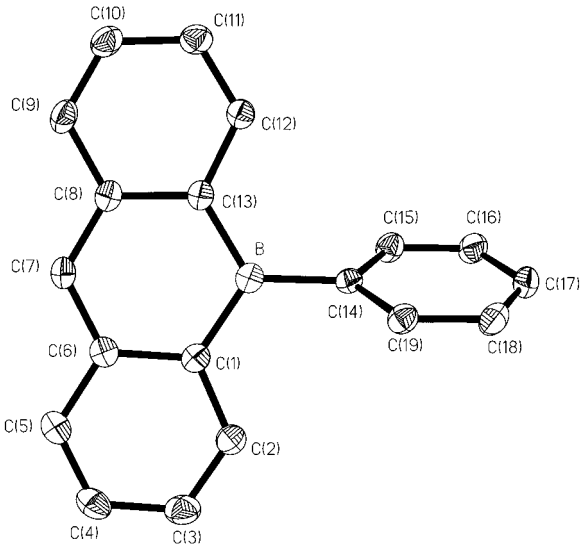

Figure 1. ORTEP view of **6** showing the labeling scheme. Thermal ellipsoids are shown at the 30% probability level.

thracene, X = Cl (**4**), Me (**5**)). These metallocene mimics can be activated toward olefin polymerization and isomerization, and the resulting catalytic behavior is described. Finally, a comparison of the reactivity of **4** with that of the non-benzannulated complex, $[C_5H_5B\text{-}Ph]Cp^*ZrCl_2$ (**8**), is made to evaluate the ligand steric effects in dictating catalyst selectivity and stability.

Results and Discussion

Ligand Synthesis. The synthesis of lithium 9-phenyl-9-borataanthracene (**3**·Li(THF)$_3$) begins with the nearly quantitative formation of 9-phenyl-9,10-dihydro-9-boraanthracene (**6**) from the reaction of 9,9-dimethyl-9,10-dihydro-9-stannaanthracene[29] with $PhBCl_2$ (eq 1). The success of the transmetalation is highly dependent on the purity of the stannaanthracene. It is best to isolate and purify the stannacycle by chromatography using silica and 6:1 hexanes/CH_2Cl_2 as the eluent.

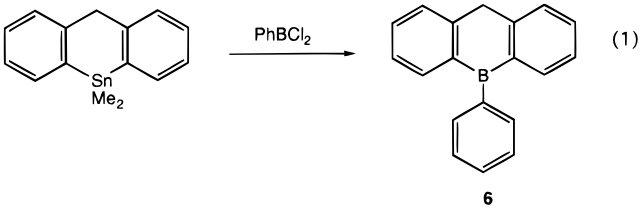

(1)

Single crystals of **6** suitable for X-ray diffraction studies were obtained by recrystallization from diethyl ether. As shown in Figure 1, the anthracene ring system is planar. The sums of all angles at the ring fusions and at boron equal 360.0(2)°. The intra-ring B−C bond lengths in **6** (mean 1.555(3) Å) are shorter than the exocyclic B−C bond (1.575(3) Å), and all three bonds are slightly shorter than the average B−C bond length found in Ph_3B (1.577(6) Å).[30] The pendant phenyl ring is not coplanar with the anthracene unit but is skewed with a 62° torsion angle. Presumably, this minimizes van der Waals repulsions between the ortho hydrogens of the phenyl ring and those at the 1- and 8-positions of the borataanthracene ring system. Thus, optimum overlap between the p orbital on B and the π electron system of the phenyl ring does not occur.

The deprotonation of **6** to yield **3**·Li(THF)$_3$ is readily achieved using the bulky base, LiTMP (TMP = 2,2,6,6-tetramethylpiperidide), in THF as shown in eq 2. The resulting tacky orange solid was characterized by standard spectroscopic and elemental analyses, and the results are consistent with its formulation. One diagnostic feature in the ^{1}H NMR (in C_6D_6) spectrum is the sharp singlet located at 7.36 ppm due to the C-10 hydrogen. In comparison, the C-10 methylene protons in **6** appear farther upfield at 4.14 ppm. The deshielding of the C-10 carbon observed in the ^{13}C NMR spectrum (**3**·Li(THF)$_3$, 101.0 ppm; **6**, 38.5 ppm) is also consistent with a change in hybridization upon deprotonation. Insofar as the ring current effect is evidence for aromaticity,[31] it can be inferred from the spectroscopic data that there is delocalization of the π-electrons within the borataanthracene moiety. Furthermore, the ^{11}B NMR of **3**·Li(THF)$_3$ shows a broad peak at 39.7 ppm (59.9 ppm for **6**), which is well within the range of values observed for other boratabenzene anions.[22,23]

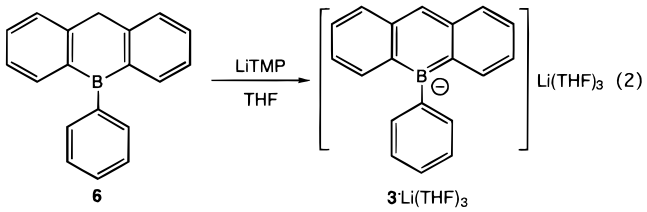

(2)

In our hands, the deprotonation of **6** with *t*-BuLi/hexane/THF to produce **3**·Li(THF)$_{3.5}$, as reported in the literature,[25] gave an intractable, oily mixture of products. A pair of well-separated multiplets which had been assigned previously to the C-10 hydrogen were consistently observed at 4.01 ppm in the ^{1}H NMR spectra of these mixtures. The higher quality of our spectra shows that these signals display geminal coupling (J = 19 Hz) and correspond to *two* protons by integration. In addition, the previously reported ^{11}B NMR value of −10 ppm has been questioned,[32] since it suggests quaternization at boron rather than deprotonation. We believe that the *t*-BuLi transfers hydride to the boron atom, forming a borate species.[33] Consistent with this idea is the B−H coupling of J = 69 Hz observed in the ^{11}B NMR spectra.

One THF solvate molecule can be removed from **3**·Li(THF)$_3$ by repeated cycles of trituration in pentane and drying under vacuum. This procedure affords **3**·Li(THF)$_2$ as a yellow powder which is more suitable for handling. The spectroscopic features of both species are almost identical.

(28) Our numbering scheme for the boraanthracene ring is shown below. It is consistent with previous assignments but differs from that of dibenzo-[*b*,*e*]borin in the following: *Ring Systems Handbook;* ACS Publications: Columbus, OH, 1993. The carbon in the 5-position is referred to as C-5 in the text. The atomic-numbering scheme used in the X-ray crystallographic studies is arbitrary, and the numerals are enclosed in parentheses, i.e. C(5).

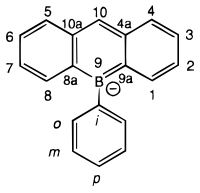

(29) Jutzi, P. *Chem. Ber.* **1971**, *104*, 1455.

(30) Zettler, F.; Hausen, H. D.; Hess, H. J. *J. Organomet. Chem.* **1974**, *72*, 157.

(31) Lowry, T. H.; Richardson, K. S. *Mechanism and Theory in Organic Chemistry*; Harper & Row: New York, 1987.

(32) Ander, I. In *Comprehensive Heterocyclic Chemistry*; Katritzky, A. R., Rees, C. W., Eds.; Pergamon Press: Oxford, U.K., 1984; Vol. 1.

(33) Hydride transfer from *t*-BuLi to boron is a well-known process. See: (a) Nöth, H.; Taeger, T. *J. Organomet. Chem.* **1977**, *142*, 281. (b) Brown, H. C.; Kramer, G. W.; Hubbard, J. L.; Krishnamurthy, S. *J. Organomet. Chem.* **1980**, *188*, 1.

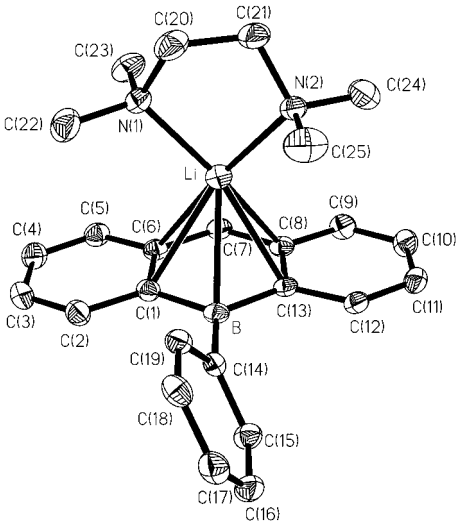

Figure 2. ORTEP view of **3**·Li(TMEDA) showing the labeling scheme. Thermal ellipsoids are shown at the 30% probability level.

Yellow needles of **3**·Li(TMEDA) (TMEDA = *N*,*N*,*N*′,*N*′-tetramethylethylenediamine) precipitate within 10 min when a solution of **3**·Li(THF)$_2$ or **3**·Li(THF)$_3$ in benzene is treated with 1 equiv of TMEDA (TMEDA = *N*,*N*,*N*′,*N*′-tetramethylethylenediamine) (eq 3). These crystals are marginally soluble in benzene, and the ^{1}H NMR spectrum of a saturated solution of **3**·Li(TMEDA) is similar to those of **3**·Li(THF)$_2$ and **3**·Li(THF)$_3$.

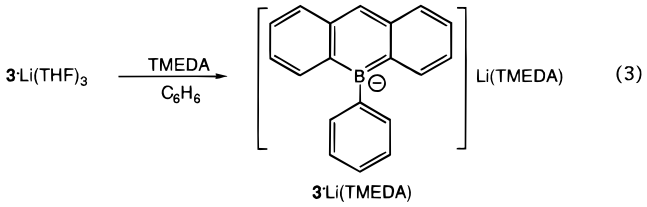

(3)

The structure of **3**·Li(TMEDA), shown in Figure 2, was determined by single-crystal X-ray diffraction. There are several variations between the structures of **3**·Li(TMEDA) and **6** (see Table 1). As expected on the basis of gained aromaticity, there is a decrease in the C(6)−C(7) and C(7)−C(8) bond lengths (from 1.506(3) to 1.409(3) Å), and the C(6)−C(7)−C(8) angle increases from 118.4(2)° to 123.2(2)°. While the carbon−carbon bond lengths of the central ring are comparable (mean 1.428(3) Å), those of the outer rings clearly exhibit single- and double-bond character (in Å: C(8)−C(9) = 1.435(3), C(9)−C(10) = 1.356(3), C(10)−C(11) = 1.409(3), C(11)−C(12) = 1.363(3)). Thus, the borataanthracene anion can be described as an aromatic boratabenzene flanked by two "diene" units. A similar bonding description can be inferred from the structural data of the 2-boratanaphthalene anion, where the boron-containing ring is aromatic while the carbocyclic ring is diene-like.[34] The lithium atom in **3**·Li(TMEDA) is η^6-bound, at least in the solid state, and it lies above the central ring of borataanthracene, being only marginally displaced from the centroid of the ring toward C(7). The structures of [3-*t*-Bu-5-MeC$_5$H$_3$BNMe$_2$][Li(TMEDA)][23c] and the Li[C$_5$H$_5$BH]$_2$ anion[23d] reveal a similar juxtaposition of the alkali metal atom. The torsion angle between the pendant phenyl ring and the borataanthracene unit remains invariant relative to **6**, and this structural feature further establishes that participation of the exocyclic substituent in donating electron density to the boron atom is minimal.

(34) For the structure of the 2-boratanaphthalene anion, see: Paetzold, P.; Finke, N.; Wennek, P.; Schmid, G.; Boese, R. *Z. Naturforsch.* **1986**, *41b*, 167. For a discussion of aromaticity in anthracene, see: (a) Schleyer, P. v. R.; Maerker, C.; Dransfeld, A.; Jiao, H.; Hommes, N. J. R. v. E. *J. Am. Chem. Soc.* **1996**, *118*, 6317. (b) Krygowski, R. M.; Cyranski, M. *Tetrahedron* **1996**, *52*, 1713. (c) Schleyer, P. v. R.; Jiao, H. *Pure Appl. Chem.* **1996**, *68*, 209.

Table 1. Selected Interatomic Distances (Å) and Bond Angles (deg) for **6** and **3**·Li(TMEDA)

	6	**3**·Li(TMEDA)
A. Interatomic Distances (Å)		
B−C(1)	1.552(3)	1.532(3)
B−C(13)	1.549(3)	1.549(3)
B−C(14)	1.575(3)	1.582(3)
C(1)−C(6)	1.408(2)	1.444(3)
C(6)−C(7)	1.506(3)	1.409(3)
C(7)−C(8)	1.506(3)	1.409(3)
C(8)−C(9)	1.396(2)	1.435(3)
C(8)−C(13)	1.404(2)	1.448(3)
C(9)−C(10)	1.375(3)	1.356(3)
C(10)−C(11)	1.388(3)	1.409(3)
C(11)−C(12)	1.376(3)	1.363(3)
C(12)−C(13)	1.410(2)	1.431(3)
B. Bond Angles (deg)		
C(1)−B−C(13)	117.8(2)	115.9(2)
C(1)−B−C(14)	120.8(2)	122.0(2)
C(13)−B−C(14)	121.3(2)	122.1(2)
B−C(1)−C(2)	122.7(2)	123.2(2)
B−C(1)−C(6)	119.8(2)	119.7(2)
C(2)−C(1)−C(6)	117.6(2)	116.9(2)
C(1)−C(6)−C(5)	119.8(2)	118.5(2)
C(1)−C(6)−C(7)	121.9(2)	120.7(2)
C(5)−C(6)−C(7)	118.2(2)	120.8(2)
C(6)−C(7)−C(8)	118.4(2)	123.2(2)
C(7)−C(8)−C(9)	117.8(2)	120.9(2)
C(7)−C(8)−C(13)	122.4(2)	120.4(2)
C(9)−C(8)−C(13)	119.8(2)	118.7(2)
B−C(13)−C(8)	119.6(2)	120.2(2)
B−C(13)−C(12)	122.9(2)	123.4(2)
C(8)−C(13)−C(12)	117.4(2)	116.6(2)

Coordination to Zirconium. The reaction of **3**·Li(THF)$_2$ with Cp*ZrCl$_3$ in toluene followed by extraction with CH$_2$Cl$_2$ affords (AnB-Ph)Cp*ZrCl$_2$ (**4**) in 44% yield as bright orange microcrystals (eq 4). Recrystallization from CH$_2$Cl$_2$/pentane

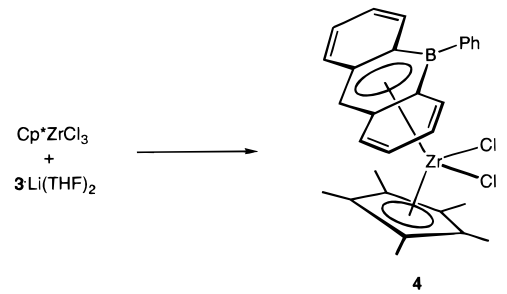

(4)

gave suitable crystals for a single-crystal X-ray diffraction study. As seen in Figure 3, this novel compound resembles a bent metallocene with a pseudotetrahedral ligand arrangement about zirconium. The centroid−Zr−centroid angle is 138.4(2)°. An examination of the structural parameters associated with **3**·Li(TMEDA) indicates that ligation to zirconium imposes distinct structural changes. The three rings of the borataanthracene unit are no longer coplanar in **4**, and in fact, the outer rings are bowed away from the Cp*ZrCl$_2$ fragment and deviate from the mean plane of the central heterocyclic ring by approximately 16°. The net effect is to reduce friction between the borataanthracene and the pentamethylcyclopentadienyl ligands.

Alkylation of **4** is complicated by boron's susceptibility to nucleophilic attack. This problem has been noted previously

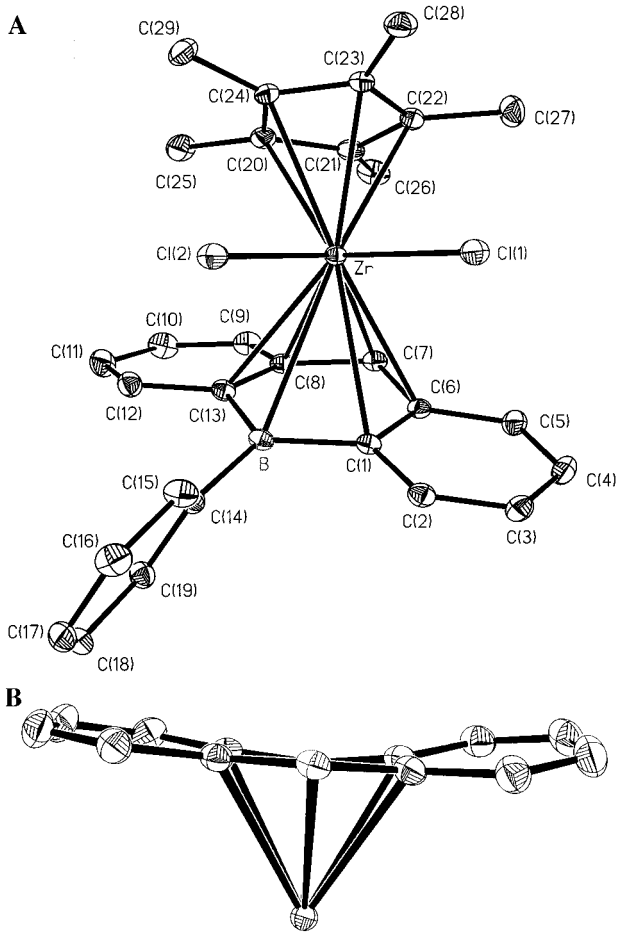

Figure 3. ORTEP view of (AnB-Ph)Cp*$ZrCl_2$ (**4**) showing the labeling scheme. Thermal ellipsoids are shown at the 30% probability level. Selected bond distances in Å: Zr−B, 2.882(2); Zr−Cl(1), 2.4260(4); Zr−Cl(2), 2.4443(4); B−C(14), 1.579(2); Zr−C(1), 2.787(2); Zr−C(6), 2.676(2); Zr−C(7), 2.472(2); Zr−C(8), 2.697(2); Zr−C(13), 2.747(2). The inset shows the bending of the borataanthracene ligand. The remaining ligands about Zr have been omitted for clarity.

for **1** and **2**, and is documented to be a function of the boron substituent.[18a] We have obtained the yellow dimethyl derivative, (AnB-Ph)Cp*$ZrMe_2$ (**5**), in 70% yield by the reaction of Cp*$ZrMe_2Cl$ with **3**·$Li(THF)_2$ in toluene (eq 5).

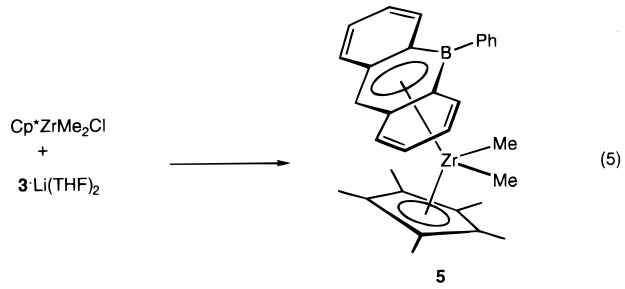

(5)

5

Following the protocol developed by Marks and co-workers for group 4 metallocenes,[4c] the treatment of **5** with one equivalent of the methide abstracting reagent, $B(C_6F_5)_3$, in CD_2Cl_2 produces [(AnB-Ph)Cp*ZrMe][$MeB(C_6F_5)_3$] (**7** in eq 6) cleanly and quantitatively by ^1H and ^{13}C NMR spectroscopies. The pertinent spectroscopic features include (1) the low-field shift of the Zr−*Me* resonance to 0.85 ppm, (2) a broad B−*Me* peak at 0.48 ppm, and (3) two signals in the ^{11}B NMR spectrum at 4.8 ppm (An*B*−Ph) and −12.9 ppm (*B*−Me). The ^{19}F NMR spectrum of **7** is unexceptional, displaying the expected three

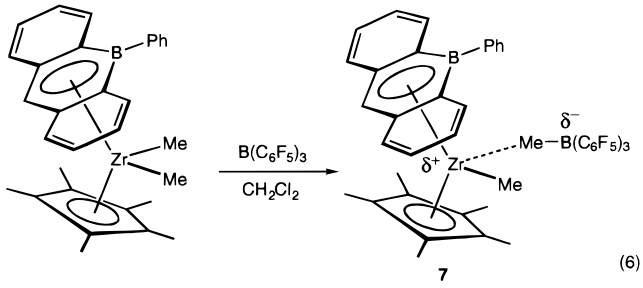

7 (6)

resonances of the $B(C_6F_5)_3$ fragment. All attempts to isolate pure **7** were frustrated by its oily nature.

It is interesting to note that the two sides of the borataanthracene ligand in **7** (i.e., the two diene fragments) are equivalent by ^1H NMR spectroscopy. Two separate exchange mechanisms have been identified for group 4 metallocenium ions generated with $B(C_6F_5)_3$: (1) ion-pair dissociation/reorganization, which involves the site exchange of the Zr−Me group in the equatorial plane of the metallocene, and (2) intermolecular Zr−Me/B−Me exchange.[4c] Similar processes may be occurring with **7**. In the ion-pair dissociation/reorganization exchange, cleavage of the weakly bound Zr···$MeB(C_6F_5)_3$ bridge results in the formation of a solvent-caged or solvent separated ion-pair, **B**. Upon recombination, the Zr-bound methyl group exchanges sites, forming either **A** or **C** (eq 7). This process exchanges

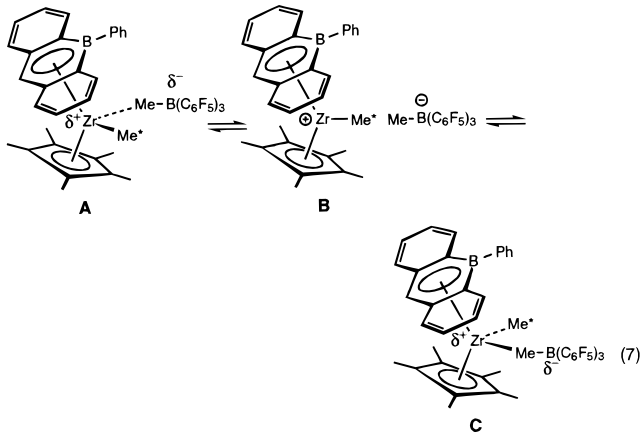

(7)

the diastereotopic sides of the π-bound ligand(s). The two sides of the borataanthracene ligand remain equivalent, even at temperatures as low as −100 °C.[35] We propose that **7** exists as a discrete ion-pair structure such as **B** in eq 7. This is quite conceivable, as the large borataanthracene and Cp* ligands should promote cation/anion separation.[36] Also, it has been shown that the activation barrier for site exchange is lowered and that the rate of dissociation is accelerated in solvents of high dielectric constant.[37] Note that the ^1H NMR signal of *Me*B-$(C_6F_5)_3$ at 0.48 ppm in **7** is typical for compounds in which the anion is free.[38] Although the exact structural composition of **7** remains unclear, and in particular, the ^{11}B signal of the borataanthracene fragment appears surprisingly upfield, the

(35) We have recently isolated and have obtained a crystal structure of the analogous cationic complex [(C_5H_5B-Ph)Cp*ZrMe][$MeB(C_6F_5)_3$]. The kinetics of the site exchange process have been measured for this complex, and we have obtained activation parameters which are comparable to those observed for standard group 4 metallocenium ions. These results will be disclosed in a future communication.

(36) Siedle, A. R.; Newmark, R. A. *J. Organomet. Chem.* **1995**, *497*, 119.

(37) Deck, P. A.; Marks, T. J. *J. Am. Chem. Soc.* **1995**, *117*, 6128.

(38) Guo, Z.; Swenson, D. C.; Guram, A. S.; Jordan, R. F. *Organometallics* **1994**, *13*, 766.

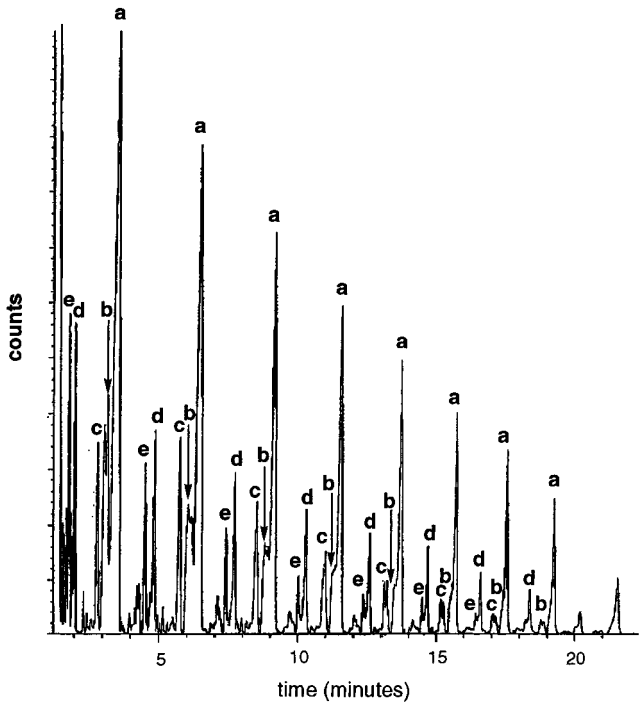

Figure 4. GC trace of the product from the reaction of **4**/1000 MAO with 1 atm of C_2H_4. Major distribution, even-carbon: (a) 2-alkenes, (b) 1-alkenes, (c) 2-alkyl-1-alkenes. Minor distribution, odd-carbon: (d) 2-alkenes, (e) 1-alkenes.

formation of **7** from $B(C_6F_5)_3$ and **5** can be reversed by using a suitable methyl source. Thus, when solutions of **7** are treated with 2 equiv of Cp_2ZrMe_2, one obtains **5** as well as the expected products from Cp_2ZrMe_2 and $B(C_6F_5)_3$.[39]

Activation and Catalytic Activity Toward Olefins. The electronic and structural similarities of **4** and **5** to group 4 metallocenes are obvious, and they suggest that these complexes may serve as precatalysts for olefin polymerization. In this section, we report on the activation of **4** and **5** and the reactivity of the catalytic species toward ethylene and 1-alkenes. It is also possible to study the reactivity of the well-defined species, **7**. Finally, a comparison between catalysts containing the [AnB-Ph]Cp* and [C_5H_5B-Ph]Cp* ligand sets highlights the role of sterics in determining the stability of this class of compounds.

An exothermic, steady uptake of ethylene is observed when 1 atm of ethylene is introduced over a toluene solution of **4** and MAO ([Zr] = 9.3×10^{-4} M, [Al] = 0.9 M); however, no polymer precipitates. Quenching the reaction and workup gives a waxy solid. The *olefinic* peaks in the ^{1}H NMR spectrum of the product reveals a composition of 47% 2-alkenes (5.39 ppm), 38% 1-alkenes (5.80 ppm (X), and 4.93 ppm (AB)), and 15% 2-alkyl-1-alkenes (4.66 ppm (s)) (eq 8).

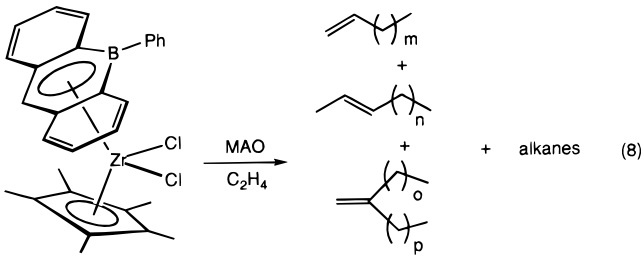

(8)

GC/MS analysis proved useful in determining the exact constitution of these olefins. Figure 4 shows the GC trace obtained from the product mixture using **4**/1000 MAO/C_2H_4. Since peak areas are proportional to the total ion count, with heavier hydrocarbons yielding higher trace abundances, the GC/MS data do not quantify the relative product ratio. However, it is clear that there are two distributions corresponding to even-carbon and odd-carbon olefin products. The most abundant distribution in Figure 4 consists of an envelope of, in order of increasing retention time, even-carbon 2-alkyl-1-alkenes (labeled as **c** in Figure 4), 1-alkenes (labeled **b**), and 2-alkenes (labeled **a**) in the range of C_{10} to C_{24}. Each set of three olefins are separated by 28 mass units, corresponding to an inserted ethylene molecule. The components of the odd-carbon distribution (**d** and **e** in Figure 4) are also separated by 28 mass units. The peaks of the two distributions are interspersed such that the overall trace shows a progression of olefin products of increasing mass (C_{10}, C_{11}, C_{12}, etc.). For a series of reactions using **4**/1000 MAO/C_2H_4, the activities over a period of 30 min lay in the range 1170−1200 kg/(mol of Zr·h).

The product distribution from the **4**/MAO/C_2H_4 reaction is complicated because there is more than one reaction path which the 1-alkenes follow after their formation and because of the statistical nature of the propagation sequence. In addition, there is also evidence for alkane formation. To clarify the fate of 1-alkenes formed by **4**/MAO/C_2H_4, we chose to react 1-tridecene directly.[40]

The ^{1}H NMR spectrum of product mixture from the slow addition of 1-tridecene to **4**/MAO ([Zr] = 9.9×10^{-4} M, [Al] = 0.9 M) in toluene shows only two *olefinic* products, 2-tridecene (74%) and 2-methyl-1-tridecene (26%).[41] Figure 5a shows the GC trace of this product mixture. The two peaks are assigned to 2-tridecene (overlaps with tridecane, total 80%) and 2-methyl-1-tridecene (20%). The product mixture is different when neat 1-tridecene is injected rapidly into the reaction solution. In addition to 2-tridecene and 2-methyl-1-tridecene, 2-undecyl-1-pentadecene (tridecene dimer) is also formed. Figure 5b shows the GC trace from the latter reaction (2-tridecene and tridecane, 80%; 2-methyl-1-tridecene and 2-methyltridecane, 14%; 2-undecyl-1-pentadecene, 6%).

Scheme 1 shows a plausible reaction sequence that accounts for the fate of 1-tridecene. Insertion of the alkene into [Zr]−H ([Zr]−H = $[(AnB\text{-}Ph)Cp^*Zr{-}H]^+$)[42] gives alkyl species, **A**. Since we know that the reaction with ethylene gives low molecular weight oligomers, while keeping a high rate of ethylene consumption, the rate of β-hydrogen elimination from **A** is faster than those in typical metallocenes. When the concentration of 1-tridecene is high, **A** can be trapped to give the disubstituted alkyl, **B**. β-Hydrogen elimination from **B** gives 2-undecyl-1-pentadecene and regenerates [Zr]−H. The formation of 2-tridecene is the result of a 2,1-insertion of 1-tridecene into [Zr]−H to give the secondary alkyl, **C**, followed by β-hydrogen elimination. Once formed, 2-tridecene does not re-enter the reaction cycle.

The presence of 2-methyl-1-tridecene and tridecane in the product mixture is best accommodated by invoking alkyl exchange between Zr and the Al in MAO. Thus, [Zr]−R (where R = H or tridecyl) reacts with an Al−Me functionality to give [Zr]−Me. Insertion of 1-tridecene into [Zr]−Me gives **D**, affording 2-methyl-1-tridecene upon β-hydrogen elimination. Tridecane is the hydrolysis product of Al−R when R = tridecyl.

(39) Bochmann, M. B.; Lancaster, S. J. *Angew. Chem., Int. Ed. Engl.* **1994**, *33*, 1634.

(40) Reactions carried out using 1-hexene and 1-octene gave the same type of products, but product isolation from the solvent was not practical.

(41) The ^{1}H NMR and GC/MS data have been compared to those of an authentic sample of 2-methyl-1-tridecene (see the Experimental Section).

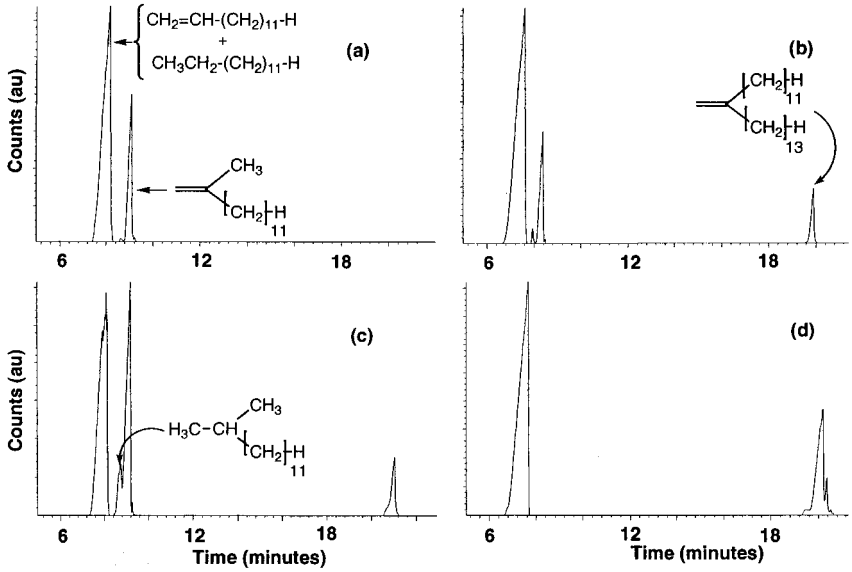

Figure 5. GC traces of the products from the reactions of 1-tridecene with (a) **4**/1000 MAO, [Al] = 0.93 M, slow addition, (b) **4**/1000 MAO, [Al] = 0.93 M, rapid addition, (c) **1**/1000 MAO, [Al] = 3.1 M, and (d) **7**.

Scheme 1

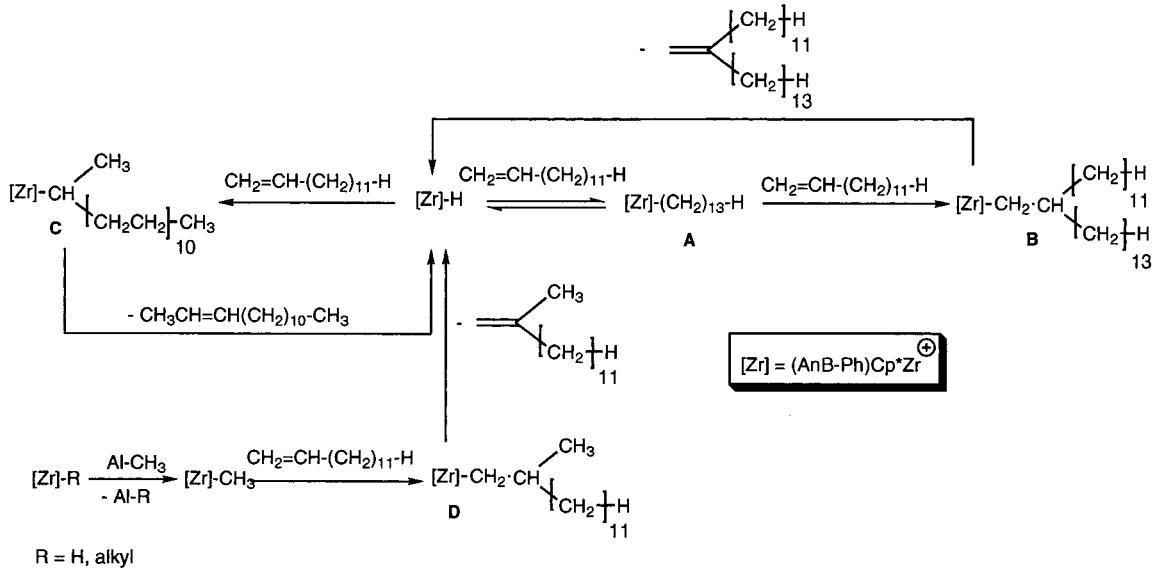

Similarly, 2-methyltridecane results from transmetalation from **D** to Al−Me, followed by hydrolysis of the resulting aluminum alkyl.

Adding 1-tridecene to solutions of **4** and MAO at higher Al concentrations results in a higher proportion of transmetalation products. For example, when [Zr] = 5.7×10^{-3} M and [Al] = 3.1 M, the rapid injection of 1-tridecene produces 2-tridecene (44%, ^{1}H NMR spectroscopy), 2-methyl-1-tridecene and 2-methyltridecane (42%), and 2-undecyl-1-pentadecene (14%) (Figure 5c).

Reactivity of [(AnB-Ph)Cp*ZrMe][MeB(C_6F_5)$_3$] (7). Precipitation of polyethylene is observed when one atmosphere of ethylene is introduced above a solution of **7** ([Zr] = 9.3×10^{-4} M). Standard workup gave soft, pliable material, corresponding to an activity over a period of 30 min of 150 kg of PE/(mol of Zr·h). The melting point of this material determined by DSC methods is 113 °C, with M_n = 50 900 and M_w = 108 000, as determined by GPC, relative to polystyrene. This information, coupled with ^{13}C NMR analysis of the product (in 1,2,4-trichlorobenzene/10% C_6D_6: δ 38.8, 37.1, 38.0, methine carbons; δ 34.3, 27.3, 30.6, methylene carbons α, β, and γ to the methine junction, respectively),[43] indicates that the polymer has a branched structure. The reaction of 1-tridecene and **7** in CD_2Cl_2 was too fast to monitor by ^{1}H NMR spectroscopy. The spectrum shows that 2-tridecene and 2-undecyl-1-pentadecene are formed in a 3:1 ratio. The GC trace of this product mixture is shown in Figure 5d.

Synthesis of (C_5H_5B-Ph)Cp*ZrCl_2 (8) and Reactivity of 8/MAO Toward Olefins. The reaction of [C_5H_5B-Ph]Li with Cp*ZrCl_3 in Et_2O affords [C_5H_5B-Ph]Cp*ZrCl_2 (**8**)[44] as a bright yellow solid (eq 9).

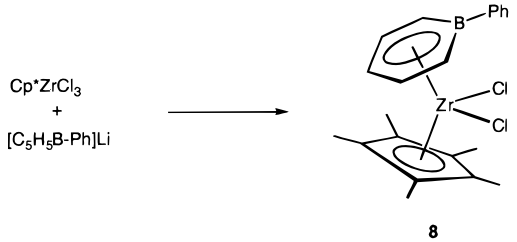

(9)

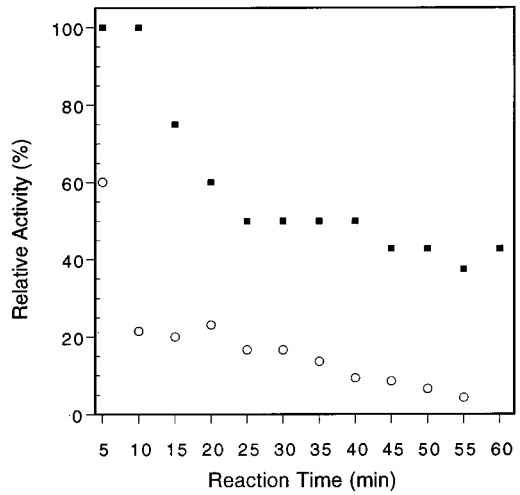

Figure 6. Rates of C_2H_4 uptake during ethylene polymerization reactions using **4**/MAO (■) and **8**/MAO (○).

The reaction of 1 atm of ethylene with **8**/1000 MAO ([Zr] = 8.9×10^{-4} M) gives polyethylene (T_m = 128 °C by DSC, M_w = 31 300, M_n = 6290 by GPC). The ^{13}C NMR (in 1,2,4-trichlorobenzene/10% C_6D_6) spectrum of this sample displays a single peak at 30.1 ppm, indicating that linear polyethylene is formed. Multiple runs gave an average activity over a 30-min period of 290 ± 5 kg of PE/(mol of Zr·h). This activity is considerably lower than that observed using **4**/MAO. The slow addition of 1-tridecene to **8**/MAO gives a product containing approximately 79% 2-undecyl-1-pentadecene, 11% 2-methyl-1-tridecene, and only 2% 2-tridecene.

Relative Stability of Catalytic Species. To establish the relative stabilities of the catalytic species, the rates of ethylene consumption throughout the course of identical polymerization reactions using **4**/MAO and **8**/MAO were measured. A comparison of the activities is illustrated in Figure 6 where the relative activity is plotted against reaction time (see the Experimental Section). The reaction using **4**/MAO is characterized by a strong C_2H_4 uptake during the initial stages of the reacton. This activity gradually levels off to about 42% of the initial uptake. Lower ethylene uptake is observed for **8**/MAO, and the activity decreases sharply as the reaction proceeds. Note that, after 60 min, ethylene consumption has nearly ceased for **8**/MAO whereas the activity of **4**/MAO is sustained. These reaction profiles indicate that the active species derived from **4**/MAO is more stable under these reaction conditions than that derived from **8**/MAO and suggest that the larger borataanthracene ligand confers significant steric stabilization.

Summary and Conclusion

We have shown that the borataanthracene framework can be used as a ligand for zirconium. The solid-state molecular structures of **6**, **3**·Li(TMEDA), and **4** give good insight into the effects of coordination and charge on the borataanthracene heterocycle. In all cases, the angle between the pendant phenyl ring and the inner core of the borataanthracene fragment remains nearly invariant at 62°. In structurally characterized [4-*t*-BuC_5H_4B-Ph]$_2ZrCl_2$,[18b] there is a nearly coplanar relationship between the boratabenzene and the pendant phenyl rings. Overall, this suggests that the steric environment around borataanthracene may not allow for optimum orbital overlap between boron and its substitutent and that the effect of the exocyclic substituent in modulating the electron density at the metal will be less pronounced than that attained in boratabenzene analogues. The severe bending of the outer rings away from the [Cp*$ZrCl_2$] core in **4** also reflects the spatial requirements of the borataanthracene ligand.

The rate of monomer uptake by **4**/MAO is among the highest observed thus far at 1 atm by a catalyst supported with boratacyclic ligands (in kg/(mol of Zr·h): **4**/MAO, 1170−1200 vs **1**/MAO, 197; **2**/MAO, 1144).[45] However, poor selectivities are observed in the reactions of **4**/MAO and ethylene, as shown in Figure 4. Since low molecular weight species are obtained, the rate of β-hydrogen elimination from the growing chain must be fast, and similar fast rates of β-hydrogen elimination have been observed with catalysts derived from [C_5H_5B-R]$_2ZrCl_2$ and MAO (R = Ph,[18b] OEt[46]).

Reactions with 1-tridecene are useful in elucidating the fate of the 1-alkenes which form in the ethylene reactions. Formation of 2-tridecene is favored under dilute conditions, and this is likely a consequence of a 2,1-insertion/β-hydrogen elimination sequence. Similar specificity for 2-alkenes results when **4**/MAO reacts with ethylene. Higher concentrations of 1-tridecene allow for double insertion (**A** to **B** in Scheme 1), ultimately making 2-undecyl-1-pentadecene. Transmetalation reactions from [Zr]−R to Al−Me functionalities in the MAO generate [Zr]−Me and lead to the formation of 2-methyl-1-tridecene.

The observation of **7**, together with its reactivity and its relationship to the well-defined group 4 metallocene catalysts, is an important step in confirming that the replacement of cyclopentadienyl ligands with boratacyclic counterparts leads to catalysts of similar overall structure. Also relevant in this context is that the reaction of **7** toward 1-tridecene leads to a similar product distribution as that with 1-tridecene and **4**/MAO. There are some notable differences between the two catalysts. Ethylene is consumed at significantly higher rates with **4**/MAO (1170−1200 kg/(mol of Zr·h) vs 150 kg/(mol Zr·h) for **7**), and the average molecular weight of the resulting ethylene oligomers is lower. In addition, the catalytic lifetime of **7** is shorter than that of **4**/MAO. These differences may be the result of different counteranion properties and the more stringent conditions for monomer purity required by **7**.[47] However, at this stage, it is not possible to rule out exchange reactions between MAO and the borataanthracene boron or the participation of byproducts from the MAO activation which have catalytic activities of their own.

The increased longevity of the catalytic species formed by **4**/MAO, relative to **8**/MAO, confirms our expectation that the larger borataanthracene ligand more effectively stabilizes a reactive metal center. This difference in size between the boratacyclic ligands may also be used to account for the different selectivities observed for **4**/MAO and **8**/MAO. Double insertion of 1-tridecene to give the β-disubstituted alkyl (*i.e.*, **B** in Scheme 1) appears to be more favored with **8**/MAO, as would be expected within a more open coordination environment. For **4**/MAO, a consecutive insertion seems disfavored on steric

(42) It is assumed in these reactions that MAO alkylates the metal and removes one ligand heterolytically to give a cationic zirconium species. See refs 3 and 4.

(43) Randall, J. C.; Hsieh, E. T. *Macromolecules* **1982**, *15*, 1402.

(44) This compound has been synthesized independently by Ashe and co-workers: Ashe, A. J., III. Private communication.

(45) These activity values differ from previously reported values because a new batch of MAO with improved properties is now commercially available. Bazan, G. C.; Lee, R. A.; Rogers, J. S. Unpublished results.

(46) Rogers, J. S.; Bazan, G. C.; Sperry, C. K. *J. Am. Chem. Soc.* **1997**, *119*, 9305.

(47) For the dependence of reactivity on counteranion properties in other catalytic systems, see: (a) Chien, J. C. W.; Song, W.; Rausch, M. D. *J. Polym. Sci., Part A.: Polym. Chem.* **1994**, *32*, 2387. (b) Siedle, A. R.; Lamanna, W. M.; Newmark, R. A. *Makromol. Chem., Macromol. Symp.* **1993**, *66*, 215. (c) Reference 9b.

grounds, and most of the reaction is channeled to the 2-tridecene product via 2,1-insertion.

These novel compounds are interesting as they show catalytic potential. Further modifications of the borataanthracene ligand (for instance, changing the substitutent on boron) or the synthesis of bis(borataanthracene)zirconium complexes may lead to new catalyst precursors which display improved product selectivities. However, the preparation of the borataanthracene framework remains, to date, synthetically demanding, and more practical syntheses need to be developed before it can be adopted as a ligand for routine use.

Experimental Section

General Methods. All manipulations were performed under an inert atmosphere using standard glovebox and Schlenk techniques.[48] Solvents were degassed and distilled from the appropriate drying agents (Et_2O, THF, C_6H_6, toluene, and pentane from sodium−benzophenone; CH_2Cl_2 and $CHCl_3$ from CaH_2). Deuterated solvents obtained from Cambridge Isotope Laboratories (all ≥99 atom % D) were treated similarly. $PhBCl_2$ (Alfa) and *n*-BuLi and $[Ph_3PCH_3]Br$ (Aldrich) were used as received. TMEDA, 1-hexene, 1-octene, 1-tridecene, and 2-tridecanone (Aldrich) were degassed and dried over molecular sieves prior to use. Cp^*ZrCl_3,[49] Cp^*ZrMe_2Cl,[50] LiTMP,[51] **6**,[29] and $[C_5H_5B\text{-}Ph]Li$[21] were prepared according to literature procedures. $B(C_6F_5)_3$ was received as a gift from Exxon Chemicals and was sublimed prior to use. MAO (9.6 wt % Al, $d = 0.88$ g/mL) was purchased from Akzo Chemicals Inc. Ethylene (Aldrich) was purified using an Oxiclear disposable gas purifier (also available from Aldrich). ^{1}H NMR (400 MHz), ^{13}C NMR (100 MHz), and ^{11}B NMR spectra (128 MHz) were recorded on a Bruker AMX-400 spectrometer, while ^{19}F NMR (473 MHz) spectra were recorded on a Varian INOVA-500 spectrometer. Chemical shifts for ^{1}H NMR and ^{13}C NMR were referenced to internal solvent resonances. Those for ^{11}B NMR and ^{19}F NMR were referenced to external $BF_3{\cdot}OEt_2$ and α,α,α-trifluorotoluene, respectively. GC/MS data were collected on a HP 5890 Series II gas chromatograph coupled with a HP 5970 Series mass selective detector. Differential scanning calorimetry measurements were performed on a TA Instruments DSC 2920 Modulated DSC. Elemental analyses were performed by Desert Analytics Laboratories, Tucson, AZ.

[AnB-Ph]Li(THF)$_3$ (3·Li(THF)$_3$). To a solution containing 1.00 g (3.93 mmol) of **6** in 10 mL of THF at −35 °C was added 0.58 g (3.9 mmol) of LiTMP in 10 mL of THF. The reaction was stirred for 4 h. Removal of volatiles under vacuum afforded **3**·Li(THF)$_3$ as a tacky orange solid (1.83 g, 97%). ^{1}H NMR (C_6D_6): δ 8.64 (d, 2H, $J = 8.2$ Hz, H_1, H_8), 8.03 (dd, 2H, $J = 7.9$, 1.4 Hz, *o*-H), 7.84 (d, 2H, $J = 7.8$ Hz, H_4, H_5), 7.60 (app t, 2H, $J = 7.8$ Hz, *m*-H), 7.44 (tt, 1H, $J = 7.4$, 1.4 Hz, *p*-H), 7.37 (ddd, 2H, $J = 7.9$, 6.5, 1.6 Hz, H_3, H_6), 7.36 (s, 1H, H_{10}), 7.00 (ddd, 2H, $J = 7.9$, 6.6, 1.3 Hz, H_2, H_7), 2.83 (m, 12H), 1.06 (m, 12H). ^{13}C {^{1}H} NMR (C_6D_6): δ 139.3 (C_{4a}, C_{10a}), 137.2 (C_1, C_8), 135.4 (C_4, C_5), 127.1 (*p*-C), 125.7 (C_3, C_6), 117.1 (C_2, C_7), 101.0 (C_{10}), 67.5 (CH_2CH_2O), 25.2 (CH_2CH_2O), *o*-, *m*-C not observed. ^{11}B{^{1}H} NMR (C_6D_6): δ 39.7. Anal. Calcd ($C_{31}H_{38}BLiO_3$): C, 78.16; H, 8.04. Found: C, 78.04; H, 7.79.

[AnB-Ph]Li(THF)$_2$ (3·Li(THF)$_2$). The **3**·Li(THF)$_3$ prepared as described above was repeatedly triturated with pentane and then filtered until the orange color in the washings no longer persisted. Drying under vacuum afforded a finely divided yellow powder. ^{1}H NMR (C_6D_6): δ 8.60 (d, 2H, $J = 8.0$ Hz, H_1, H_8), 7.99 (d, 2H, $J = 6.8$ Hz, *o*-H), 7.81 (d, 2H, $J = 8.4$ Hz, H_4, H_5), 7.60 (t, 2H, $J = 7.5$ Hz, *m*-H), 7.44 (t, 1H, $J = 7.2$ Hz, *p*-H), 7.37 (t, 2H, $J = 7.0$ Hz, H_3, H_6), 7.29 (s, 1H, H_{10}), 7.00 (t, 2H, $J = 7.2$ Hz, H_2, H_7), 2.37 (m, 12H), 0.80 (m, 12H). ^{13}C{^{1}H} NMR (C_6D_6): δ 139.0 (C_{4a}, C_{10a}), 136.9 (C_1, C_8), 135.4 (C_4, C_5), 128.9 (br, C_{8a}, C_{9a}), 127.4 (*o*-C), 127.1 (*p*-C), 126.9 (*m*-C), 125.6 (C_3, C_6), 116.9 (C_2, C_7), 101.0 (C_{10}), 67.6 (CH_2CH_2O), 25.0 (CH_2-CH_2O). ^{11}B{^{1}H} NMR (C_6D_6): δ 39.8. Anal. Calcd ($C_{27}H_{30}BLiO_2$): C, 80.22; H, 7.48. Found: C, 79.60; H, 7.33.

[AnB-Ph]Li(TMEDA) (3·Li(TMEDA)). A 50.0-mg (0.124-mmol) sample of **3**·Li(THF)$_2$ was dissolved in 1 mL of benzene. To this solution was added 19.0 μL (0.126 mmol) of TMEDA. After stirring for 10 min, the orange solution turned bright yellow, and microcrystalline material precipitated. Recrystallization was induced by warming the solution to 60 °C and allowing it to cool gradually, whereupon yellow crystals of **3**·Li(TMEDA) formed. The crystals were washed with cold pentane and collected by filtration (35 mg, 75%). ^{1}H NMR (C_6D_6): δ 8.63 (d, 2H, $J = 8.1$ Hz, H_1, H_8), 7.98 (d, 2H, $J = 6.8$ Hz, *o*-H), 7.80 (d, 2H, $J = 8.5$ Hz, H_4, H_5), 7.59 (app t, 2H, $J = 7.6$ Hz, *m*-H), 7.44 (t, 1H, $J = 7.4$ Hz, *p*-H), 7.36 (ddd, 2H, $J = 7.8$, 6.8, 0.9 Hz, H_3, H_6), 7.29 (s, 1H, H_{10}), 7.00 (ddd, 2H, $J = 7.9$, 6.5, 1.4 Hz, H_2, H_7), 1.00 (s, 12H), 0.96 (s, 4H). ^{13}C{^{1}H} NMR (C_6D_6): δ 139.0 (C_{4a}, C_{10a}), 137.3 (C_1, C_8), 135.5 (C_4, C_5), 127.6 (*o*-C), 127.5 (*p*-C), 127.2 (*m*-C), 125.8 (C_3, C_6), 117.5 (C_2, C_7), 101.1 (C_{10}), 55.5 (CH_2NMe_2), 43.7 ($CH_2N\mathit{Me}_2$). ^{11}B{^{1}H} NMR (C_6D_6): δ 39.8. Anal. Calcd (C_{25}-$H_{30}BLiN_2$): C, 79.80; H, 8.04; N, 7.44. Found: C, 79.66; H, 7.80; N, 7.43.

(AnB-Ph)Cp*ZrCl$_2$ (4). A solution of 100 mg (0.247 mmol) of **3**·Li(THF)$_2$ in 10 mL of toluene was added to a rapidly stirred slurry containing 82 mg (0.25 mmol) of Cp^*ZrCl_3 in 10 mL of toluene at −35 °C. The reaction mixture was allowed to stir for 8 h. The solvent was removed, and the residue was extracted with CH_2Cl_2. The extract was filtered and reduced in volume. Recrystallization by vapor diffusion of pentane into the CH_2Cl_2 extract afforded **4** as orange microcrystals. A second crop of crystals could be obtained by concentration of the mother liquor and vapor diffusion with additional pentane (total yield, 60 mg, 44%). ^{1}H NMR (CD_2Cl_2): δ 8.07 (d, 2H, $J = 7.8$ Hz, H_1, H_8), 7.68 (d, 2H, $J = 8.2$ Hz, H_4, H_5), 7.68 (d (overlaps with H_4, H_5), 2H, *o*-H), 7.54 (ddd, 2H, $J = 8.2$, 6.8, 1.4 Hz, H_3, H_6), 7.47, (app t, 2H, $J = 7.8$ Hz, *m*-H), 7.40 (m, 3H, H_2, H_7, *p*-H), 7.00 (s, 1H, H_{10}), 1.90 (s, 15H). ^{13}C{^{1}H} NMR (CD_2Cl_2): δ 139.3 (C_1, C_8), 136.4 (C_{4a}, C_{10a}), 134.1 (C_4, C_5), 132.2 (C_3, C_6), 127.1 (*o*-C), 127.0 (*p*-C, 126.9 (*m*-C), 126.0 (C_5Me_5), 125.0 (C_2, C_7), 93.8 (C_{10}), 12.5 ($C_5\mathit{Me}_5$). ^{11}B{^{1}H} NMR (CD_2Cl_2): δ 49.5. Anal. Calcd ($C_{29}H_{29}BCl_2$-Zr): C, 63.27; H, 5.31. Found: C, 63.13; H, 5.17.

(AnB-Ph)Cp*ZrMe$_2$ (5). A mixture of 100 mg (0.247 mmol) of **3**·Li(THF)$_2$ and 72 mg (0.25 mmol) of Cp^*ZrMe_2Cl was dissolved in 25 mL of cold (−35 °C) toluene. After stirring for 4 h, the solvent was evaporated, and the crude product was extracted with pentane. The extract was filtered, reduced in volume, and allowed to stand at −35 °C overnight, whereby **5** precipitated as yellow flakes (122 mg, 70%). ^{1}H NMR (CD_2Cl_2): δ 8.07 (d, 2H, $J = 8.2$ Hz, H_1, H_8), 7.71 (br, 2H, *o*-H), 7.48 (m, 4H, H_4, H_5, *m*-H), 7.42 (tt, obscured, $^3J_{HH} = 1.4$ Hz, *p*-H), 7.40 (ddd, 2H, $J = 8.2$, 6.7, 1.5 Hz, H_3, H_6), 7.25 (ddd, 2H, $J = 8.0$, 6.8, 1.2 Hz, H_2, H_7), 6.61 (s, 1H, H_{10}), 1.72 (s, 15H), −1.15 (s, 6H). ^{13}C{^{1}H} NMR (CD_2Cl_2): δ 138.6 (C_1, C_8), 136.0 (C_{4a}, C_{10a}), 134.9 (C_4, C_5), 130.9 (C_3, C_6), 127.7 (*o*-C), 127.4 (*p*-C), 127.2 (*m*-C), 123.0 (C_2, C_7), 119.2 (C_5Me_5), 93.4 (C_{10}), 44.0 (ZrMe), 12.0 ($C_5\mathit{Me}_5$). ^{11}B{^{1}H} NMR (CD_2Cl_2): δ 46.2. Anal. Calcd ($C_{31}H_{35}BZr$): C, 73.06; H, 6.71. Found: C, 72.79; H, 6.75.

[(AnB-Ph)Cp*ZrMe][MeB(C$_6$F$_5$)$_3$] (7). A solution containing 49 mg (0.096 mmol) of $B(C_6F_5)_3$ in 5 mL of CH_2Cl_2 was cooled to −35 °C. This was slowly added to a stirred solution containing 50 mg (0.098 mmol) of **5** in 5 mL of CH_2Cl_2 at −35 °C. The yellow solution turned bright magenta then dark purple. ^{1}H NMR (CD_2Cl_2): δ 8.11 (tt, 1H, $J = 7.2$, 1.2 Hz, *p*-H), 7.95 (d, 2H, $J = 8.1$ Hz, H_1, H_8), 7.91 (d, 2H, $J = 8.0$ Hz, *o*-H), 7.86 (app t, 2H, $J = 7.1$ Hz, *m*-H), 7.59 (ddd, 2H, $J = 8.2$, 7.1, 1.1 Hz, H_3, H_6), 7.40 (ddd, 2H, $J = 8.1$, 7.1, 1.0 Hz, H_2, H_7), 7.33 (d, 2H, $J = 8.2$ Hz, H_4, H_5), 6.02 (s, 1H, H_{10}), 1.43 (s, 15H, Cp*), 0.85 (s, 3H, ZrMe), 0.48 (br s, 3H, BMe). ^{13}C{^{1}H} NMR (CD_2Cl_2, −70 °C): δ 155.4 (C_{4a}, C_{10a}), 147.2 (d, $^1J_{CF} = 234$ Hz), 138.6 (C_1, C_8), 136.6 (d, $^1J_{CF} = 242$ Hz), 136.3 (C_4, C_5), 135.8 (C_3, C_6), 135.5 (d, $^1J_{CF} = 244$ Hz), 132.1 (C_2, C_7), 129.8 (*o*-C), 129.7 (*p*-C), 128.1 (*m*-C), 126.9 (C_5Me_5), 106.6 (C_{10}), 16.6 (Zr-Me), 10.5 ($C_5\mathit{Me}_5$), 8.9 (B-Me). ^{11}B{^{1}H} NMR (CD_2Cl_2): δ 4.8 (An*B*), −12.9 (*B*-Me). ^{19}F NMR (CD_2Cl_2): δ 70.5 (d, $J = 19.8$ Hz, *o*-F), 38.6 (t, $J = 20.3$ Hz, *p*-F), 36.0 (t, $J = 21.8$ Hz, *m*-F).

(48) Burger, B. J.; Bercaw, J. E. In *Experimental Organometallic Chemistry*; Wayda, A. L., Darensbourg, M. Y., Eds.; ACS Symposium Series 353; American Chemical Society: Washington, DC, 1987.
(49) Wolczanski, P. T.; Bercaw, J. E. *Organometallics* **1982**, *1*, 793.
(50) Rodriguez, G. Ph.D. Thesis, University of Rochester, 1997.
(51) Olofson, R. A.; Dougherty, C. M. *J. Am. Chem. Soc.* **1973**, *95*, 581.

[C_5H_5B-Ph]Cp*$ZrCl_2$ (8). Approximately 10 mL of Et_2O was vacuum transferred into a flask containing 100 mg (0.625 mmol) of [C_5H_5BPh]Li and 208 g (0.625 mmol) of Cp*$ZrCl_3$ at −78 °C. The pale yellow slurry was allowed to warm to room temperature and was stirred overnight. The solvent was removed, and the residue was extracted with toluene. The extract was filtered and reduced in volume, and the addition of pentane caused the precipitation of a yellow solid. This solid was washed with pentane and recrystallized from toluene/pentane (1:2 v/v) (240 mg, 85%). ^{1}H NMR (C_6D_6): δ 8.05 (d, 2H, J = 6.8 Hz, *o*-H), 7.42 (t, 2H, J = 7.4 Hz, *m*-H), 7.30 (t, 1H, J = 7.3 Hz, *p*-H), 7.16 (m, 2H, CHC*H*CHB), 6.83 (d, 2H, J = 9.2 Hz, CHCHC*H*B), 5.69 (t, 1H, J = 6.8 Hz, C*H*CHCHB), 1.68 (s, 15H). ^{13}C{^{1}H} NMR (C_6D_6): δ 142.9 (CHC*H*CHB), 134.0 (*o*-C), 129.3 (*p*-C), 128.1 (*m*-C), 126.7 (br, CHCH*C*HB), 126.1 (C_5Me$_5$), 108.5 (*C*HCHCHB), 12.5 (C_5*Me*$_5$). ^{11}B{^{1}H} NMR (C_6D_6): δ 41.2. Anal. Calcd ($C_{21}H_{25}BCl_2Zr$): C, 56.00; H, 5.59. Found: C, 54.26; H, 5.60.

Ethylene Polymerization Reactions. The following description is representative. A 7.03-g aliquot (25.0 mmol of Al) of MAO was weighed into a 100-mL round-bottomed flask. With rapid stirring, a 14-mg sample (0.025 mmol, Zr/Al ratio = 1/1000) of **4** dissolved in 5.0 mL of toluene was added to the MAO solution, followed by 15.0 mL of toluene as diluent. The flask was fitted with a Teflon inlet adapter, and the entire assembly was weighed. The flask was immersed in a 21 °C constant-temperature bath, and after evacuation for 15 s, ethylene (1 atm) was introduced into the reaction vessel. After a reaction time of 30 min, the flask was closed off from the ethylene source, and the assembly was reweighed. The flask was then opened to air, and the solution was quenched with distilled water. A 5-mL aliquot of the reaction mixture was drawn for ^{1}H NMR and GC/MS analyses. The remaining solution was stirred into 3 M NaOH until the aluminum salts dissolved completely. The remaining polymer was collected by vacuum filtration, washed with distilled water, and dried under vacuum.

Reactions with 1-Alkenes. The procedure described using 1-tridecene is representative. The catalyst solution was prepared as described for the polymerization reactions. A 1.0-mL toluene solution containing 100 mg of 1-tridecene was added dropwise into the catalyst solution over a period of 20 min. Alternatively, neat substrate was injected rapidly into the catalyst solution. After a total reaction time of 30 min, the reaction was quenched with water. The organic layer was separated from the aqueous layer, and toluene was removed by rotary evaporation to afford 87 mg of product.

Ethylene Polymerization with 7. A 15.0-mg (0.0293-mmol) sample of B(C_6F_5)$_3$ dissolved in 15.0 mL of toluene was added to 14.9 mg (0.0292 mmol) of **5** in 15.0 mL of toluene at −35 °C. After the mixture was stirred for 5 min, the flask was fitted with a Teflon inlet adapter and the entire assembly was weighed. The flask was immersed in a 21 °C constant-temperature bath and partially evacuated for 15 s, and ethylene (1 atm) was introduced into the reaction vessel. Following a reaction time of 30 min, the flask was closed off from the ethylene source and the assembly was reweighed. A 5-mL aliquot of the reaction solution was drawn for ^{1}H NMR and GC/MS analysis. The catalyst was quenched by the addition of 5 mL of water, and the polymer was isolated by removal of volatiles in vacuo.

Reaction of 7 with 1-Tridecene. A 10.0-mg (0.0195-mmol) sample of B(C_6F_5)$_3$ dissolved in 10.0 mL of toluene was added to 10.0 mg (0.0196 mmol) of **5** in 11.0 mL of toluene at −35 °C. After stirring for 5 min, 35.8 mg (0.196 mmol) of 1-tridecene was added dropwise to the stirred solution. After 30 min, the reaction was quenched with 1 mL of water. The organic layer was separated off, and 32.0 mg of the product was isolated by removal of toluene by rotary evaporation.

Measurement of Ethylene Consumption. Each catalyst solution was freshly prepared prior to the activity measurement: (1) A solution containing 9.0 mg of **4** in 5.0 mL of toluene was added dropwise with stirring to 4.60 g of MAO. An additional 13.1 mL of toluene was added to the catalyst solution as diluent. (2) In the same manner, a toluene solution containing 7.4 mg of **8** and 4.60 g of MAO was prepared in a separate reaction vessel ([Zr] = 8.9×10^{-4} in each catalyst solution).

The reaction vessel was fitted with a Teflon inlet adapter. A specially designed mineral oil bubbler equipped with a calibrated flow tube was attached to the vent of the ethylene manifold. The reaction vessel was attached to the vacuum line between the ethylene source and the vent. For an uptake measurement, the ethylene source was closed, and the time (to the nearest 1 s) required for the oil to rise up the length of the flow tube (corresponding to a volume of 0.8 mL) was recorded. Measurements were taken at 5-min intervals for a period of 1 h. Measuring uptake times more precisely, especially at the intial stages of the reaction where ethylene consumption is extremely fast, is difficult, thereby introducing a margin of error in the measurement. The rates of ethylene consumption in Figure 6 were normalized against the maximum activity of the **4**/MAO catalyst system.

Preparation of 2-Methyl-1-tridecene. A 16.7-mL aliquot of *n*-BuLi (26.7 mmol, 1.6 M in hexanes) was added dropwise to a stirred solution containing 9.50 g (26.6 mmol) of Ph_3PCH_3Br in 60 mL of THF at −78 °C. After 30 min, the reaction was brought to 0 °C and was allowed to stir at this temperature for an additional 1 h. A mixture containing 5.28 g (26.6 mmol) of 2-tridecanone in 10 mL of THF was slowly added to the flask, and the reaction was allowed to stir overnight, during which time a white precipitate formed. The solution was filtered through Celite, and the filter cake was washed with pentane. The combined filtrate and washings were removed in vacuo to afford a yellow residue. The residue was extracted with pentane, and crude 2-methyl-1-tridecene was isolated upon evaporation of pentane. Pure product (5.02 g, 96%) was obtained by vacuum distillation (55 °C, 0.01 Torr). ^{1}H NMR ($CDCl_3$): δ 4.66 (s, 1H), 4.64 (s, 1H), 1.98 (t, 2H, J = 7.6 Hz), 1.69 (s, 3H), 1.40 (br, 2H), 1.24 (s, 16H), 0.86 (t, 3H, J = 6.8 Hz), −0.62 (s, 6H). ^{13}C{^{1}H} NMR ($CDCl_3$): δ 146.2, 109.5, 37.9, 32.0, 29.8, 29.7, 29.6, 29.4, 29.4, 27.7, 22.4, 14.1. MS: M^+ 196, calcd for $C_{14}H_{28}$ 196.4.

Structure Determination of 3·Li(TMEDA), 4, and 6. X-ray quality crystals of **3**·Li(TMEDA) were grown from a benzene solution which was slowly cooled from 60 °C to room temperature. Crystals of **4** were grown from methylene chloride vapor diffused with pentane at −35 °C. Crystals of **6** were grown from diethyl ether at −35 °C. Fragments of **3**·Li(TMEDA), **4**, and **6** were cut and mounted on glass fibers under Paratone-8277 and were placed on the X-ray diffractometer in a cold nitrogen stream supplied by a Siemens LT-2A low-temperature device. The X-ray intensity data were collected on a standard Siemens SMART CCD area detector system equipped with a normal focus molybdenum-target X-ray tube operated at 2.0 kW (50 kV, 40 mA) for **3**·Li(TMEDA) and **4** and at 1.5 kW (50 kV, 30 mA) for **6**. A total of 1.3 hemispheres of data were collected using a narrow frame method with scan widths of 0.3° in ω and exposure times of 10 s/frame for **3**·Li(TMEDA), **4**, and **6**. Frames were integrated to 0.75 Å for **3**·Li(TMEDA) and **6** and to 0.90 Å for **4** with the Siemens SAINT program yielding a total of 7896 reflections for **3**·Li(TMEDA), 28 688 reflections for **4**, and 14 650 for **6**. The unit cell parameters were based upon the least-squares refinement of three-dimensional centroids of 2448 reflections, 5424 reflections, and 1849 reflections at −80, −90, and −50 °C for **3**·Li(TMEDA), **4**, and **6**, respectively. The space groups were assigned on the basis of sytematic absences and intensity statistics by using the XPREP program (Siemens, SHELXTL 5.04). The structures of **3**·Li(TMEDA) and **4** were solved by direct methods (SHELXTL program, version 5.04) and were refined by full-matrix least-squares on F^2. The structure of **6** was solved using MITHRAL-88 (TEXSAN-92). All non-hydrogen atoms for the structures were refined with anisotropic thermal parameters, giving a data-to-parameter ratio of >10:1 for both **3**·Li(TMEDA) and **4**. H atoms were included in idealized positions for the structures. Selected bond distances and angles for **3**·Li(TMEDA) and **6** are provided in Table 1 in the text.

Acknowledgment. G.C.B. is an Alfred Sloan Fellow and a Henry and Camille Dreyfus Teacher Scholar. The authors are grateful to these agencies for financial assistance and to the anonymous reviewers for helpful suggestions. We are also grateful to Thomas Mourey (Eastman Kodak Co.) for the GPC data.

Supporting Information Available: Complete crystallographic studies for complexes **3**·Li(TMEDA)**, 4,** and **6** (34 pages, print/PDF). See any current masthead page for ordering information and Web access instructions.

JA972651+